HHS Public Access

Author manuscript

Cancer Lett. Author manuscript; available in PMC 2022 May 28.

Published in final edited form as:

Cancer Lett. 2021 May 28; 506: 142–151. doi:10.1016/j.canlet.2021.01.020.

Physical Confinement during Cancer Cell Migration Triggers Therapeutic Resistance and Cancer Stem Cell-like Behavior

Qionghua Shen[1], **Tamara Hill**[1], **Xue Cai**[2], **Loan Bui**[3], **Rami Barakat**[1], **Emily Hills**[1], **Turki Almugaiteeb**[4], **Anish Babu**[5], **Patrick H Mckernan**[5], **Michelle Zalles**[6], **James D Battiste**[5,*], **Young-Tae Kim**[1,7,*]

[1]Neuroengineering Lab, Department of Bioengineering, University of Texas at Arlington, TX

[2]Department of Neurosurgery, University of Oklahoma Health Sciences Center, OK

[3]Department of Aerospace & Mechanical Engineering, University of Notre Dame, IN

[4]RPD Innovations, Riyadh, Saudi Arabia

[5]Department of Neurology, University of Oklahoma Health Sciences Center, OK

[6]Oklahoma Medical Research Foundation, OK

[7]Department of Urology, UT Southwestern Medical Center, TX

Abstract

Metastasized cancer cells have an increased resistance to therapies leading to a drastic decrease in patient survival rates. However, our understanding of the cause for this enhanced resistance is lacking. In this study, we report that physically tight confinement during cancer cell migration triggers therapeutic resistance and induces cancer stem cell-like behavior including up-regulation in efflux proteins and in cancer stem cell related markers. Moreover, the re-localization of Yes-associated protein (YAP) to the cell nucleus indicated an elevated level of cytoskeletal tension. The increased cytoskeletal tension suggested that mechanical interactions between cancer cells and tight surroundings during metastasis is one of the factors that contributes to therapeutic resistance and acquisition of cancer stem cell (CSC) like features. With this system and supporting data, we are able to study cells with therapeutic resistance and CSC-like properties for the future purpose of developing new strategies for the treatment of metastatic cancer.

[*]Correspondence and Requests for materials should be addressed to: Young-Tae Kim, Ph.D., Department of Bioengineering, 500 UTA Blvd ERB244, University of Texas at Arlington, Arlington, TX 76010, ykim@uta.edu, Fax : 817-272-2251, Phone: 682-559-9003, James D. Battiste, M.D., Ph.D., Department of Neurology, 920 Stanton L. Young Blvd, Suite, 2040, University of Oklahoma Health, Science Center, Oklahoma City, OK 73104, James-Battiste@ouhsc.edu, Fax: 405-271-5723, Phone: 405-271-4113.

7. Author Contributions

Y.T.K. and J.D.B. were the principal investigators and conceived the idea. Q.S., T.H. and X.C. wrote the paper. Q.S. and T.H. developed the idea and designed the experiments. Y.T.K. and L.B. designed the microchannel devices. Q.S. provided all G55 data. T.H. provided all MDA-MB-231 data. X.C. and J.D.B. carried out all radiation experiments. R.B. provided A549 data and E.H. provided PC3 data.

Declaration of Interests

All authors declare that there is no competing financial interests or personal relationships that could have appeared to influence the work reported in this paper.

Keywords

cancer metastasis; physical confinement; therapeutic resistance

1. INTRODUCTION

More than 90% of mortality caused by cancer is attributable to metastases [1, 2]. Due to its unique systemic nature and resistance to existing therapeutic agents, metastatic cancer is largely incurable with current common treatments [1, 3].

Cancer cell migration is a key element of the invasion-metastasis cascade; the extraordinary motility and deformability of metastatic migrating cells allow them to easily move through physical confinement [4, 5]. During this process, cells undergo a change known as metastatic resistance [6]. Although the major mechanisms of resistance have been widely investigated, the relationship between migration in physical confinement and the procurement of therapeutic resistance is not well elucidated. In addition, a rare population of tumor cells with stem cell-like properties, labeled as cancer stem cells (CSCs), can play a distinct role in driving metastasis. CSCs are difficult to study because of their small number within the tumor population. Previous works have suggested that CSC initiation and maintenance may be related to physical inputs such as extracellular matrix stiffness within the local microenvironments [7, 8]. Hence, mechanical inputs such as interstitial pressure from the microenvironment, might greatly affect the CSC-like behaviors of cancer cells and drive metastatic invasion. A critical step to improve our understanding of the mechanisms underlying treatment resistance is to generate appropriate tools with physical inputs to induce or enrich for treatment resistant cancer cells.

In this study, we produced a group of confined-migrating cancer cells by allowing them to migrate in a physically confined microenvironment (i.e., a microchannel with a width that is smaller than the cells size); and carried out detailed molecular analyses on those confined-migrating cancer cells to establish the relationship between mechanical interaction and acquired therapeutic resistance. This study focuses on G55 glioblastoma and MDA-MB-231 breast cancer cell lines. The aim of this study is to confirm that physical confinement induces chemotherapeutic and radio-therapeutic resistance. Detailed protein level comparison was used to determine which molecules are potential key players for physical confinement induced therapeutic resistance by Western blot analysis. Immunostaining and hypoxic analysis further allowed us to evaluate the relationship between cytoskeletal pressure, CSC-like properties and physical confinement induced therapeutic resistance. We also found a similar phenomenon (i.e., physical confinement induces therapeutic resistance) in lung, prostate, and patient-derived GBM. Thus, we believe this physical confinement induces therapeutic resistance as a universal trait in various cancer types.

2. Materials and Methods

2.1 Fabrication of Microchannel Devices

Two different styles of microchannel devices described in our previous studies were used for this study (demonstrated in supplemental information Fig. S1. A and B) [9]. Combined utilization of standard negative photolithography and soft lithography was the core of our microchannel device fabrication, with recessed features fabricated on a silicon wafer coated with SU-8 photoresist (Microchem Corp, Newton, MA). The thickness of coating was controlled by spin speed which determined the microchannels' height. A mixture of polydimethylsiloxane (PDMS) (Sylgard 184 Silicone Elastomer Base, Dow Corning) and curing agent (Sylgard 184 Silicone Elastomer Curing Agent, Dow Corning) in a ratio of 10:1 (v/v) was poured over the completed master and pre-baked for 2 minutes at 75°C, then solidified for 5 minutes at 150°C. Subsequently the peeled PDMS devices with the designed microchannels were carefully cut, decontaminated with 70% ethanol, and assembled.

2.2 Cancer Cell Culture

The human glioblastoma cell line G55 was provided by The University of Oklahoma Health Sciences Center. The cells were cultured in a serum-free DMEM/F-12 medium supplemented with 1x B-27 (Invitrogen), 1x Insulin-Transferrin-Selenium-X (Invitrogen), and mouse EGF (epidermal growth factor, 20ng/ml, PeproTech). MDA-MB-231 human breast carcinoma cells were provided by The University of Texas Southwestern Medical Center in Dallas. The cells were cultured in DMEM/F-12 medium (Corning/Cellgro) supplemented with 10% fetal bovine serum (FBS).

2.3 Migrating Cell Initiating and Cell Harvesting

For G55 cells, 25×10^3 cells were introduced at each side entrances of the microchannel device (totally 50×10^3 cells per device, Fig. S1. B). All devices were maintained in 10% serum medium to facilitate the initiation of adhesion and migration via confined microchannels. For MDA-MB-231 cells, before introducing the cells into the microchannel devices, 6-well plates (n=3, containing 18 independent microchannel devices, Fig. S1. B) were coated with collagen type I (Corning, REF 354236) overnight, then rinsed them with 1xPBS three times for neutralization. 100×10^3 cells were seeded into each well and cultured in 10% serum supplemented media for up to 7 days to allow from ample cells to migrate through the microchannels. The culture medium was abandoned, and the cells were washed twice with 1xPBS. Then all devices were incubated with Trypsin-EDTA for 5 minutes, with later addition of an equal volume of medium. Quickly, the bottom of the well was scraped with Cell Lifter (Corning, Costar® 3008) to remove 2D cells (i.e., cancer cells growing at the out of microchannels) and verified under the microscope to make sure there were no remaining 2D cells. The PDMS device was then peeled to expose the migrating cells. Once more, the wells were incubated with Trypsin-EDTA for 5 minutes and migrating cells were exclusively collected from 18 devices (total cell number was estimated to be 60×10^3, Fig. S3). For the control group, channel-less PDMS pieces were disassembled and cells were collected from one well after a 5-minute incubation with Trypsin-EDTA. Cells from both groups were centrifuged for 5 minutes at 4000 rmp. The supernatant was discarded, and the cell pellet was harvested for Western blot analysis.

2.4 Western blot analysis and quantification

Total cell lysates were obtained by adding RIPA buffer (R0728, Sigma-Aldrich) and protease inhibitor cocktail (P2714, Sigma-Aldrich). Equilibrated protein samples were loaded into a 10% SDS-Page gel, electrophoresed and then electro-transferred to a PVDF membrane (Bio-Rad). Transferred membranes were blocked with a blocking buffer containing 5% non-fat milk (Labscientific, M0841). The following monoclonal antibodies were used: Nanog (Cell Signaling, D73G4), CD133 (Cell Signaling, D2V8Q), CD44 (Cell Signaling, 8E2), ALDH1/2 (Santa Cruz, sc-166362), ALDH1 (Cell Signaling, D9J7R), MDR1/ABCB1 (Cell Signaling, E1Y7B), HIF1-α (Cell Signaling, D5F3M), ABCG2 (Cell Signaling, D5V2K), nucleoporin-62 (Santa Cruz, sc-48373), EpCAM (Cell Signaling, VU1D9) and EPAS-1 (Santa Cruz, 190B). Target proteins were visualized with the secondary mouse or rabbit IgG antibodies and a chemiluminescent substrate (Santa Cruz, sc-2048). All Western blot results were normalized by total protein (Fig. S5). All Western blot experiments were reproduced and performed three times for quantification.

2.5 3D Reconstruction of Migrating Cells via tightly confined microchannel

Microchannel devices (Fig. S1. A) with migrated cells were fixed using 4% paraformaldehyde for 10 minutes and perfused with washing solution (0.5% triton in 1xPBS) for 1 hour. Samples were stained with Actin-Stain™ 488 (Cytoskeleton) and 15 minutes of PI (Propidium iodide, 500nM, MP) at room temperature. Images were scanned using a z-step size of 0.5 μm. 3D reconstruction was carried out by MATLAB and ImageJ.

2.6 Immunostaining

Microchannel devices (Fig. S1. A) with a sufficient number of migrating cells were fixed using 4% paraformaldehyde for 10 minutes and washed with 1xPBS. After blocking with 4% goat serum in washing solution (0.5% triton in 1xPBS) for 1 hour, samples were immunostained with either ABCG2 (1:500, Cell Signaling, D5V2K), nucleoporin P62 (1:500, Thermo-Fisher, PA5–21882) or YAP (1: 500, Santa Cruz, sc-271134) antibody at 4°C overnight. After washing 3 times with washing solution, samples were incubated with Alexa Fluor® Goat Anti-Rabbit IgG (1:200, Jackson ImmunoResearch Laboratories) for 2 hours at room temperature. Signal visualization and image capture were performed using a ZEISS LSM 800 fluorescence microscopy. Fluorescence intensities were quantified by ImageJ. The ratio of YAP intensity between the cytoplasm and the nucleus was taken as an indicator of mechanical pressure to the cells when they traveled through the tightly confined microchannels.

2.7 Intracellular drug accumulation comparison between migrated and non-migrating cells

Devices with 5 × 5 μm microchannels (Fig. S1. A) was used to separate migrated cells from non-migrating cells. 20×10^3 cells were seeded to the central reservoir of each device and cultured for up to 6 days. Cells were classified into three different migrating status: non-migrating 2D culture cells (i.e., cells growing at the initial seeding central reservoir), migrating cells, and migrated cells (i.e., cells entered, migrated via tightly confined microchannel, and exited to the other side of reservoir) (Fig. S1. C). The cells were then

treated with naturally fluorescent Doxorubicin (Dox, 17μM, Doxorubicin hydrochloride, Sigma-Aldrich) for 4 hours at 37°C. Four hours after, Doxorubicin was removed and the cells were washed with live cell image medium (1582202, Life Technologies) and imaged to determine the intracellular accumulation of the Doxorubicin (i.e., 4 hour Dox accumulation). All samples were imaged by a ZEISS LSM 800 fluorescence microscopy using bright field and Rhodamine filter set (Dox). Cells in two different locations were imaged: central reservoir (2D control cells) and 5 × 5 reservoir (5R, cells migrated through 5 × 5 μm microchannels, Fig. 1). After taking 4 hour Dox accumulation, the cells were kept in the image medium overnight and imaged again to compare the Doxorubicin efflux between non-migrating 2D cells and migrated cells. All images were quantified for Dox fluorescence intensities at nucleus and cytoplasm by ImageJ (Fig. 1).

2.8 Viability comparison between migrating and non-migrating cells

G55 GBM cells were treated with Doxorubicin (17μM) overnight or Temozolomide (TMZ, 0.25 mM, 0.5 mM, and 1 mM, T2577, Sigma) for 72 hours at 37°C. MDA-MB-231 cells were incubated with Doxorubicin (17μM) overnight or 5-Fluorouracil (5-Fu, 25μM, Sigma-Aldrich) for 72 hours. Cell viability under various anti-cancer drug treatments was determined with the Green Live/Dead Stain (34J66, ImmunoChemistry) with 1:1,000 (v/v) in 1xPBS.

2.9 G55 Radiation and Viability Test

G55 cells were seeded at the both sides of the entrance of the microchannels (total 50×10^3 cells per device, Fig. S1. B and Fig. 2A) and incubated for 3–4 days to allow the cell migration via tightly confined microchannels. The same number of cells for the 2D cell culture were seeded in plain 6-well plates in 2 ml same media and cultured overnight. Then radiation of a single dose of 2 Gy, 5 Gy, or 10 Gy was performed with a high dose-rate ^{137}Cesium (Cs) unit (4.5 Gy/min) at room temperature [10] (Fig. 2B). To make a condition in the 2D cell culture similar to the confined-migrating cells (inside microchannel) during radiation, a PDMS cover was put on the top of each well just before radiation and was removed after radiation (Fig. 2A). Cell viability of both 2D and confined-migrating cells was assessed at 48 hours post radiation. For assay of migrating cell viability, Hoechst 33342 (0.5μg/ml, Thermo-fisher) and Propidium iodide (0.5μg/ml, MP Biomedicals) staining was carried out. Images were taken using a Nikon E-2000 fluorescence microscopy, and the nuclei (both total and dead) inside the microchannels were quantified. For assay of 2D cell viability, the media in each well were collected (to harvest the floating cells) and the adhered cells in correspondent wells were collected after Trypsin (0.25%, VWR) treatment and were added to the collected media. 10 μl of each sample were mixed with 10 μl of trypan blue stain (0.4%, Invitrogen), and 10 μl of that was used to determine the cell viability using a cell counter according to the manufacture's protocol (Invitrogen).

2.10 Mouse G55 xenograft model and brain tissue immunohistochemistry

Mouse xenograft models were established using the G55 cells that was stereotactically implanted into the striatum of a mouse brain guided by Bregma coordinates. The brain was harvested after allowing time for tumor growth/migration and then fixed with formalin and paraffin embedded (FFPE). The immunohistochemical analysis was performed on Leica

Bond RXM platform using Polymer Refine Detection system (DS9800). The collected brain tissues were sectioned at 4 μm thickness and mounted on positively charged slides. The slides were then dried overnight at room temperature and incubated at 60°C for 45 minutes. Slides were transferred to the Leica Bond RXM for dewax and then treated for target retrieval at 100°C for 20 minutes in a retrieval solution at pH 6. The sections were then incubated with 5% goat serum (01–6201, Thermo-Fisher) for 30 minutes. Endogenous peroxidase was blocked using peroxidase-blocking reagent, followed by the primary antibody (ABCG2, Abcam 207732) incubation for 60 minutes. For the secondary antibody, post-primary IgG-linker and/or Poly-HRP IgG reagents was used. Detection was done using 3, 3′-diaminobenzidine tetrahydrochloride (DAB) as chromogen and counter stained with hematoxylin. Completed brain tissue slides were dehydrated (Leica ST5020) and mounted (Leica MM24). Slides were imaged by light microscopy (Fig. 5. A3).

2.11 Determination of Hypoxia level during confined-migration

Microchannel devices with adequate number of physically confined migrating cells were incubated with the Image-iT® Hypoxia Reagent (10μM, H10498, Life Technologies) at 37°C for 30 minutes. Hypoxic visualization and image capture were performed using a ZEISS LSM 800 fluorescence microscopy under 20X with excitation/emission of 490/610nm. Fluorescent intensity in the central reservoir, inside the microchannels and the satellite reservoirs were measured by ImageJ and compared among the groups.

2.12 Reseeding experiment

For G55, after harvesting the live confined-migration cells (as described previously) from 18 devices (about 54×10^3 cells in total), the cells were reseeded in the plain 24-well plates (without microchannels) and re-cultured for 48 hours to determine whether protein expression changes induced by confined-migration persist after removal from physical confinement. For MDA-MB-231, the confined-migration cells were re-seeded in the plain 24-well plates (without microchannels) and collected at 2, 3, 4, and 8 days post seeding for Western blot analysis.

2.13 Statistical Analyses

Microsoft Excel was used to calculate the averages and standard deviations (STDs). To compare the statistical significance, a one-way ANOVA tests and Tukey post hoc tests among multiple groups and the two-tails student *t*-test were performed. A *p*-value of less than 0.05 was considered statistically significant.

3. RESULTS

3.1 Confined-migrating Cancer Cells Develop Chemotherapy and Radiotherapy Resistance

The confined-migrated cells moving through physical confinement showed characteristic resistance to chemo-therapeutic agent, Doxorubicin (Dox). Both GBM and MDA-MB-231 cancer cell lines were treated with 17μM Dox for visualization of intracellular drug mobility, due to the degree of Dox autofluorescence at this concentration [11]. After 4 hours Dox incubation, samples were imaged at two different timepoints: immediately after Dox

removal (4hr) and 16 hours (overnight). The autofluorescence of Dox in intracellular compartments (i.e., total cell, nucleus, and cytoplasm) was measured and compared. After drug treatment for 4 hours, Dox intensities in two locations (2D and 5R) showed no significant differences. However, Dox accumulation was highest at the nucleus due to DNA-Dox interaction (Fig. 1 A1 and B1). After incubating overnight with Dox free medium, the general Dox intensity was in a reducing trend due to efflux property though for 2D cells more Dox accumulated to nuclei because of DNA bonding effect of Dox. Viewed in detail, the cells which migrated through 5 × 5 μm (5R) microchannels had significantly lower concentration of Dox in all intracellular compartments compared to 2D cultured cells (Fig. 1 A2 and B2). Both G55 (Fig. 1 C) and MDA-MB-231 (Fig. 1 D) cells showed obvious changes in Dox intensity under different degrees of confinement. When comparing 4hr and overnight, we observed increased Dox intensity in the nucleus of 2D cultured cells, but the confined-migrated cells showed a significant decrease in Dox intensity. For G55 cells, there was 12% increase (2D) and 41% decrease (5R) (Fig. 1 E1). For MDA-MB-231 cells, 23% increase (2D) and 43% decrease (5R) (Fig. 1 F1). The cytoplasmic Dox intensity decreased in G55 cells (−11% for 2D and −31% for 5R cells), but the intensity increased in MDA-MB-231 (+104% for 2D and +69% for 5R). Total Dox intensity changes after overnight incubation is shown in Fig 1. E3 and F3. Based on the Dox intensity change pattern as total intensity of Dox decreased after overnight incubation, the Dox accumulation difference is mainly depending on drug efflux. To further address the implication of increased Dox efflux in the confined-migrated cells, cell viability after Dox treatment was examined: G55 cells showed 20% higher viability in the migrated group (for 5R) as compared to 2D cells (Fig. 1 G); MDA-MB-231 2D cells showed a high sensitivity to Dox (~15% viability) compared to migrated cells (~100% viability) (Fig. 1 I). These results were consistent with the pattern of Dox intensity changes under different degrees of confinement. To further confirm the confined-migration induced chemotherapeutic resistance, TMZ and 5-FU (clinically used chemotherapeutic agents) were used for G55 and MDA-MB-231, respectively. After 72 hours TMZ treatment, the viability was significantly higher for migrated cells (5R) than the 2D cells at all doses (Fig. 1 H). After 72 hours 5-FU treatment, the migrated cells showed a significantly higher (~100% in 5R) viability than 2D cells (~50%) (Fig. 1 J). Taken together, these data indicate that the confined-migrated cells have a resistance to a variety of chemotherapies and confined-migrated cells have increased drug efflux. Therefore, these results offer a mechanism by which the confined migration endows metastatic cancer cells with resistance by the increased ability to efflux drug.

To determine the characteristic radiation resistance of the confined-migrating cells and 2D cells, two groups of cells were equally irradiated with doses of 2 Gray (Gy), 5 Gy or 10 Gy, and then cell survival rates, which were normalized to the non-irradiated group, were compared among these two groups (Fig. 2 A). The data showed that at low doses (2 Gy and 5 Gy), 2D cells and the confined-migrating cells showed no significant differences in radio-sensitivity. However, the cell viability was reduced with increasing radiation dose in both groups. At the highest dose (10 Gy), the confined-migrating cells showed a significantly higher survival rate over the 2D cells (Migrating: 94.8 ± 10.1 vs. 2D: 87.8 ± 4.1, p=0.0165) (Fig. 2 B). There was no significant decrease in viability of confined-migrating cell even

after treatment with the highest dose (Figs. 2 B–C). These results confirm that the confined-migrating cells have an increased resistance to radiation.

3.2 Confined-migrating Cells Exhibit Significantly Increased Drug Efflux Proteins

In Dox accumulation studies, cells that migrated through physical confinement exhibited an increased Dox efflux as compared to 2D cultured cells. Western blot analyses revealed that the confined-migrating cancer cells up-regulated the following drug efflux proteins: ABCG2, MDR1, and nucleoporin-62 (NUP62) (Figs.3 A–E). In G55 cells, the confined-migrating cells expressed a four-fold increase in ABCG2 (Fumitremorgin C inhibiting experiment also proved ABCG2 increased in confined-migrating cells (Fig. S2)); a two-fold increase in MDR1; and a three-fold increase in NUP62 compared to 2D cultured cells (Figs. 3 A–C). Similarly, both ABCG2 and MDR1 showed increased expressions in the confined-migrating MDA-MB-231 cells as 2.5 times and 29 times respectively compared to 2D cultured cells (Figs. 3 D and E). Additionally, immunostaining revealed a higher expression of ABCG2 and NUP62 protein in G55 and MDA-MB-231 cells when they migrated through the physically confined 5 × 5 μm microchannels (Fig. 3 F). The increased drug-efflux protein expression of the confined-migrating cells contributes to higher cell viabilities due to increased drug expulsion.

3.3 Confined-migrating Cancer Cells Up-regulate CSCs Related Biomarkers in Various Cancer Types

Cancer stem cells (CSCs) is a rare population within the whole tumor population. Recent work in glioblastoma and breast cancers has pointed out that increasing CSCs population can increase the whole tumor's resistance against radiation- and chemotherapy allowing tumor to survive and recurrence [12, 13]. CSCs' resistance mechanisms include DNA damage repair, amplified checkpoint activation and expression of additional drug pumps, such as ATP-binding cassette (ABC) transporters [14–16]. Those mechanisms are exactly related to resistance to Dox and radiation therapy. Therefore, to further understand the increased therapeutic resistance after confined-migration, we examined whether the confined-migrating cancer cells exhibit cancer stem cell like properties. CD133, a biomarker for cancer stem cells, expression in confined-migrating G55 cells was increased 50% compared to 2D control (Fig. 4 A1); while CD44, another biomarker for CSCs, expression was reduced around 90% in the migrating group (Fig. 4 A2). This CD133-CD44 shift has been reported in a patient-derived glioma stem cell (GSC) cell line when cells were subject to hypoxia [17]. Aldehyde dehydrogenase (ALDH) is also frequently used to identify CSCs [18]. In this study, the confined-migrating G55 cells expressed two times ALDH (Fig. 4 A3) and four times EPAS-1, a specific marker for GSCs (Fig. 4 A4). CD133 expression in confined-migrating MDA-MB-231 cells was significantly increased by 6.2 times (Fig. 4 B1) along with other breast CSC biomarkers: ALDH (1.7 times), EpCAM (1.3 times) and Nanog (3.2 times) (Figs. 4 B2–B4).

To find out whether such increase of CSC properties in the confined-migrating cells was restricted to a certain type of cancer or is ubiquitous, several other types of cancer cells (patient-derived C25 GBM, A549 lung cancer, and PC3 prostate cancer) were tested (Figs. 4 C–E). CD133 expression in the confined-migrating cells was 16 times higher in C25 cells

(Fig. 4 C), 4 times in A549 cells (Fig. 4 D), and 5 times in PC3 cells (Fig. 4 E). These results clearly indicate that the confined-migrating cancer cells exhibit cancer stem cell like properties which could be correlated to increased therapeutic resistance.

3.4 Physical Confinement Increases Migrating Cancer Cells' Cytoskeleton Tension with Minimal Hypoxic Stress

When migrating via physically confined microchannels, cells showed different morphology due to confinement from their surroundings. Here, in order to show impacts from different degrees of confinements, we added 15 × 15 μm microchannel (Fig. 5 A1). When cancer cells migrate through a physically confined 5 × 5 μm microchannel, their nuclei were confined by the tight space such that the nuclei turned to be a specially elongated shape. Based on 3D reconstruction model we calculated the cross-section ratio (cross section acreage of cell/ cross section acreage of microchannel) for the confined-migrating cells. For 2D cells, the cross section was considered as 0. Cells migrating inside 5 × 5 μm microchannel were exposed to significantly higher confinement, shown by more than 80% cell membrane clinging to microchannel walls, than 2D or cells migrating via relatively open microchannel (15 × 15 μm) (Fig. 5 A2). This evidence is consistent with what we observed from *in vivo* model. In the G55 murine xenograft model of glioblastoma multiforme, migrating-G55 cells creeping along the cortical white matter tracts (labelled with arrowhead) demonstrated elongated morphology similar as migrating inside 5 × 5μm microchannels (Fig. 5 A3). Those elongated G55 cells also expressed higher ABCG2 compared to non-migrated G55. CD133 staining also showed higher expression in metastatic G55 under physical confinement (Supplementary data, Fig S6).

According to the above evidence, we believe while migrating in microchannels (the same as migrating in confined tissue), the cells need to overcome the resistance associated with the confinement. To assess how the microchannel's dimensions affect confinement caused by hydraulic resistance, we utilized the concept from hydrodynamics by expressing the resistance as a function of channel dimensions: height (h), width (w), and length (L) while the viscosity of the fluid (μ) is kept as constant:

$$R(Resistance) = \frac{12\mu L}{wh^3}\left[1 - \frac{192}{\pi^5}\left(\frac{h}{w}\right)\sum_{i=1,3,5}^{\infty}\frac{tanh\left(\frac{i\pi}{2}\left(\frac{w}{h}\right)\right)}{i^5}\right]^{-1}$$

[19]

To compare the resistance, three different sized microchannels were considered (5 × 5, 5 × 12 and 15 × 15μm), leading to the calculated resistances summarized in Fig. 5 A4. Considering the effective hydraulic resistance associated with the 15 × 15μm ($w \times h$) microchannel as the baseline, the effective resistance a cell needs to overcome to migrate in a 5 × 5μm cross-section is 81 times higher due to confinement. This increase suggests a much higher energetic demand from the cell to migrate through a physically confined microenvironment (by comparison, this would emulate the increased energy needed to metastasize distant brain tissue).

YAP relocation from cytoplasm to nucleus (measured as a ratio) indicates increased cytoskeleton tension due to shear force on the cell membrane [20, 21]. To investigate the relationship between confined-migrating, therapeutic resistance and CSC like behaviors, we examined Yes-associated protein (YAP) relocation and intracellular oxygen level in the different degrees of confinement. The YAP ratio was significantly increased as the microchannel width decreased in both cell types (Figs. 5 B and G). In both G55 (Fig. 5 C) and MDA-MB-231(Fig. 5 H), nuclear YAP fluorescence were evidently lower than in the cytoplasm for the 2D group, but cells that migrated through physical confinement had higher YAP fluorescence inside the nucleus. YAP fluorescence nucleus localization was consistent with 3D reconstruction results (Fig. 5 A). It proved that the confined pressing force due to the tight surroundings did increase the confined-migrating cell's intracellular skeleton tension.

Hypoxia is a well-known factor that induces cancer stem cell like variation, malignant growth, and cancer metastases [22–24]. Hypoxia-induced factor 1-alpha (HIF-1α), which is known to regulate multiple cellular activities including cell survival in hypoxic conditions and epithelial-to-mesenchymal metastatic cascades [24, 25], was up-regulated 20 times in the migrating G55 cells and 4 times in the migrating MDA-MB-231 cells (Figs. 5 F and K). To determine if HIF-1α increased due to hypoxic condition during confined migration, the intracellular oxygen level was measured by Image-iT® Hypoxia Reagent expression. Interestingly, cells in the central 2D area showed a higher fluorescence intensity compared to the cells around the microchannel entrance and those migrating via physically confined microchannels (Figs. 5 D and J). When G55 cells were close to the microchannel entrance, the fluorescence intensity dropped to 30% of the cells in the 2D center reservoir. After migrating into 5 × 5 μm microchannels, cells exhibited the lowest hypoxia dye intensity (Fig. 5 E). For MDA-MB-231 cells, when cells were close to the microchannel entrance and inside the microchannels the hypoxic dye intensity dropped to 20% of the 2D cells (Fig. 5 I). Additionally, when we compare HIF-1α expression between hypoxia cells and confined-migrating cells, around two times higher expression was observed in the confined-migrating group (Fig. S4). Based on these results, the significant increase in HIF-1α expression was not caused by a hypoxic condition during confined-migration.

3.5 Protein expression changes induced by confined-migration persist after removal from physical confinement

To determine if the protein changes induced by confined-migration remained permanently, the migrating cancer cells were collected and re-cultured on the 2D environment over different time periods. In G55 cells, expression levels of selected proteins (ABCG2, ALDH and CD44) were assessed by Western blots and compared among 2D control cells, migrating cells, and 2-day re-cultured cells. There was no significant difference in these proteins between the migrating group and the 2-day re-cultured group, but both were significantly different from 2D cultured cells (Figs. 6 A–C). Likewise, the confined-migrating MDA-MB-231 cells were collected and re-cultured for 2, 3, 4 and 8 days. Western blot results showed that cells could maintain the altered protein expression levels up to 4 days whereas, at day 8 of re-culture, all protein levels finally returned to the original baseline (Figs. 6 D–

F). Although protein changes induced by confined-migration are not permanent, the changes persist for at least 4 days.

4. DISCUSSION

Currently, treatment with radiation and chemotherapy after surgical resection to remove tumors is the standard-of-care for many cancer patients [4, 26]. However, the highly therapeutic resistant nature of metastatic cancer cells tends to limit the efficacy of current cancer treatments. A better understanding of what triggers confined-migration (via physically constricted tissue) induced resistance is important for improving anticancer strategies, specifically for metastatic cancer. In this study, we successfully isolated and examined therapeutically resistant confined-migrating cancer cells; we discovered that mechanical stimulation caused by physical confinement could be one of the factors that leads to increased resistance in migratory cells. This is accomplished by cells adjusting their membrane protein channels and up-regulating CSCs related biomarkers.

Viability studies after certain chemotherapy or radiation treatments (representative of GBM) showed confined-migrating/migrated cells to have significantly higher survival rates than 2D cultured cells. Based on these results, we confirmed cells that experience confined-migration become resistant. The drug efflux experiments support the increased viability demonstrating resistance; confined-migrated cells have lower drug accumulation compared to the control group for both cancer types due to increased drug efflux. It is well-established that cancer cells in the resistance category can change the activity and/or structure of the cell membrane in order to regulate chemical transportation [27–30]. On the cell membrane, resistance is mostly controlled by the ATP-binding cassette (ABC) transporter proteins including P-glycoprotein (ABCB1), the multidrug resistance-associated protein 1 (MRP1), MRP2 and ABCG2 [30, 31]. In the cell nucleus, resistance may be controlled by nucleoporins as the gateway that regulates the molecular exchange between the cell nucleus and the cytoplasm [32, 33]. Western blot data, showing increased expressions of ABCG2 and MDR1 on the cell membrane and NUP62 on the nuclear envelope (G55 cells in particular), were consistent with viability and drug efflux studies. These data provide evidence that confined-migration is tightly linked to up-regulation of multidrug resistance associated proteins, leading to drug resistance. Furthermore, the proliferation-inhibiting effect during confined-migration is responsible for increased radiation resistance.

Besides observing the up-regulated therapeutic resistance, we also observed molecular alterations on confined-migrating cells with implications for cancer stem cell biology. Transmembrane glycoprotein CD133 and aldehyde dehydrogenase (ALDH) are the foremost markers used in isolating stem cells from various tissues, including CSCs [18, 34, 35]. When in a confined-migrating state, both GBM and breast cancer cells showed increased CD133 and ALDH expression, indicating the acquisition of cancer stem cell-like features resulting from migration through physically tight confinement. Changes in other CSC related markers, CD44, EPAS-1 (for GBM), EpCAM, and Nanog (for breast cancer) further confirm that CSC like features can be acquired during confined-migration [36, 37]. Additionally, we observed increased expression of CD133 in several other cancer cells (A549 lung cancer, PC3 prostate cancer, and C25 patient-derived GBM), suggesting that induction of CSC-like

behaviors is not just limited to a specific cancer cell type, but possibly a feature in all migrating cancer cells. Among the changes of confined-migration induced CSCs biomarkers, we observed that CD44 and CD133 expression is inversely related in GBM: increased CD133 and decreased CD44[17]. The expression shift between CD44 and CD133 is known to be influenced by environmental factors, such as hypoxia, chemotherapy, or radiotherapy [17, 38]. The observed shift can be attributed to the confined environment experienced by migrating cells. A boosted resistance to radiation therapy is also evidence that confined-migrating cells possess CSC-like properties [39]. Taken together, we believe that physical confinement during migration can guide activation of specific intracellular cascades that induce CSC-like behaviors.

Understanding the factor(s) which trigger(s) confined-migration induced therapeutic resistance and CSC-like behavior is critical to develop therapeutic strategies for the treatment of metastatic cancer. In our study, the major difference between a confined-migrating cell and a 2D cultured cell is degree of physical confinement. Cells migrating through physical confinement have a microenvironment where their migration is confined by contacts with the surrounding structures with inherently more contact points compared to cells in 2D where cells can freely grow, proliferate, or migrate with minimal physical constraint. In order to ascertain which factor(s) trigger therapeutic resistance and cancer stem cell-like behavior during confined-migration, we investigated if the cells were experiencing hypoxia and/or shear force by interaction with their tight surroundings. HIF-1α a well-known intracellular indicator of developmental response to hypoxia, showed increased expression in confined-migrating cells. However, our hypoxic data demonstrated that cells inside the microchannels were subjected to only minimal or no hypoxic (< 5% atm O_2) conditions. The regulation of HIF-1α expression and activity is complicated and is not only up-regulated in hypoxic conditions. Apart from hypoxia, it can also be activated through an oxygen-independent manner by various cytokines through the PI3K-AKT-mTOR pathway [40], which is known to increase survival under various stress conditions [41, 42]. However, HIF-1α has been reported that is required for a high-level cell motility but is linked to a novel HIF-1α mediated signaling pathway that is independent of hypoxia [41]. As reported by Li's group, hypoxia *per se* did not influence cell migration but presenting of HIF-1α protein promoted cell migration. Combined there reported cased with our observations suggest that the lack of oxygen is not the major factor triggering therapeutic resistance in cancer cells during confined-migration. Therefore, we assert the observed treatment resistance with increased efflux proteins and up-regulation of HIF-1α and other CSC related markers, could be induced by mechanical interaction between cells and their surroundings rather than oxygen deficit. To further elucidate the role of mechanical interaction, Yes-associated protein (Yorkie-homologues YAP) whose nuclear localization property is accompanied with cells' response to a narrow ECM passageway [20], was used as a tool to demonstrate the intracellular skeletal tension caused by mechanical interaction during migration through physical confinement. It has been reported that YAP/TAZ localization is dependent on cell volume (cell shape and aspect ratio) as under confinement more YAP/TAZ relocated to nuclear [42]. Besides, YAP/TAZ activation are related to cancer stem cell attributes, cancer proliferation, chemoresistance and metastasis [43, 44]. All these are consistent with our observation that confined-migrating cancer cells with higher ratio of

YAP/TAZ nuclear localization demonstrating higher therapeutic resistance that caused by increased drug efflux proteins and CSC-like behavior. Immunohistochemical staining of ABCG2 in glioblastoma multiforme xenograft model showed that G55 cells migrating in white matter track would turn to elongated shape and demonstrated higher ABCG2 expression. This phenomenon was consistent with acquisition of drug resistance and increase in CSC related biomarker expression. Hence, we conclude that confined pressure and interaction from the surrounding environment during migration has a profound impact on cell behaviors [20, 45] and leads to up-regulated therapeutic resistance and production of CSC-like features. These features acquired during confined-migration were maintained at least for 48 hours when removed from confinement. Therefore, forcing cells to migrate through physical confinement provides a potential new avenue for obtaining multifactorial therapeutic resistant cancer cells (having increased drug efflux and CSC-like behavior). Future studies can harness this technique in the development of new anticancer treatments, specifically targeting metastatic, therapy resistant cancer.

Supplementary Material

Refer to Web version on PubMed Central for supplementary material.

Acknowledgements

We thank Dr. Kimberly Bowles, Dr. Kytai Nguyen, Dr. Yi Hong and Dr. Baohong Yuan for kindly providing us with training and facility access to conduct protein analysis. We thank Dr. Bo Chen for kindly assisted us with taking confocal images and Dr. Charles Chuong provided guidance for hydrodynamic simulation. We also thank Calvin Kong for reviewing the manuscript. Acknowledgement also goes to the University of Oklahoma Health Sciences Center for providing patient-derived cancer samples.

5. Funding

This work was supported by Cancer Prevention and Research Institute of Texas (RP150711) and Institutional Development Award from the National Institute of General Medical Sciences of the National Institutes of Health (P20GM103639).

References:

[1]. Valastyan S, Weinberg RAJC, Tumor metastasis: molecular insights and evolving paradigms, cell 147 (2011) 275–292. [PubMed: 22000009]

[2]. Gupta GP, Massagué JJC, Cancer metastasis: building a framework, 127 (2006) 679–695.

[3]. Lambert AW, Diwakar R Pattabiraman, and Robert A. Weinberg., Emerging biological principles of metastasis, Cell, 168.4 (2017) 670–691. [PubMed: 28187288]

[4]. Friedl P, Wolf K.J.N.r.c., Tumour-cell invasion and migration: diversity and escape mechanisms, 3 (2003) 362.

[5]. M. M, Cellular mechanobiology and cancer metastasis Birth Defects Research Part C: Embryo Today: Reviews, 81 (2007) 329–343.

[6]. J. MD, Mechanics & Malignancy: Physical cues and changes that drive tumor progression, Georgia Institute of Technology, (2015).

[7]. Sneddon JB, Werb Z, Location, location, location: the cancer stem cell niche, Cell stem cell, 1 (2007) 607–611. [PubMed: 18371402]

[8]. Yu H, Mouw JK, Weaver VM, Forcing form and function: biomechanical regulation of tumor evolution, Trends in cell biology, 21 (2011) 47–56. [PubMed: 20870407]

[9]. Bui LSQ, Hill T, et al., Microchannel Device for Proteomic Analysis of Migrating Cancer Cells, Biomedical Physics & Engineering Express, (2018).

[10]. Mehta M, Basalingappa K, Griffith JN, Andrade D, Babu A, Amreddy N, Muralidharan R, Gorospe M, Herman T, Ding W-Q, HuR silencing elicits oxidative stress and DNA damage and sensitizes human triple-negative breast cancer cells to radiotherapy, Oncotarget, 7 (2016) 64820. [PubMed: 27588488]

[11]. Li D, Zhang Y-T, Yu M, Guo J, Chaudhary D, Wang C-C, Cancer therapy and fluorescence imaging using the active release of doxorubicin from MSPs/Ni-LDH folate targeting nanoparticles, Biomaterials, 34 (2013) 7913–7922. [PubMed: 23886730]

[12]. Eyler CE, Rich JN, Survival of the fittest: cancer stem cells in therapeutic resistance and angiogenesis, Journal of clinical oncology: official journal of the American Society of Clinical Oncology, 26 (2008) 2839. [PubMed: 18539962]

[13]. Bai X, Ni J, Beretov J, Graham P, Li Y, Cancer stem cell in breast cancer therapeutic resistance, Cancer treatment reviews, 69 (2018) 152–163. [PubMed: 30029203]

[14]. Rich JN, Bao S, Chemotherapy and cancer stem cells, Cell stem cell, 1 (2007) 353–355. [PubMed: 18371369]

[15]. Huang EH, Heidt DG, Li C-W, Simeone DM, Cancer stem cells: a new paradigm for understanding tumor progression and therapeutic resistance, Surgery, 141 (2007) 415–419. [PubMed: 17383517]

[16]. Rich JN, Cancer stem cells in radiation resistance, Cancer research, 67 (2007) 8980–8984. [PubMed: 17908997]

[17]. Brown DV, Filiz G, Daniel PM, Hollande F, Dworkin S, Amiridis S, Kountouri N, Ng W, Morokoff AP, Mantamadiotis T, Expression of CD133 and CD44 in glioblastoma stem cells correlates with cell proliferation, phenotype stability and intra-tumor heterogeneity, PLoS One, 12 (2017) e0172791. [PubMed: 28241049]

[18]. Visvader JE, Lindeman GJ, Cancer stem cells in solid tumours: accumulating evidence and unresolved questions, Nat Rev Cancer, 8 (2008) 755–768. [PubMed: 18784658]

[19]. Olanrewaju A, Beaugrand M, Yafia M, Juncker D, Capillary microfluidics in microchannels: from microfluidic networks to capillaric circuits, Lab on a Chip, 18 (2018) 2323–2347. [PubMed: 30010168]

[20]. Dupont S, Morsut L, Aragona M, Enzo E, Giulitti S, Cordenonsi M, Zanconato F, Le Digabel J, Forcato M, Bicciato S, Role of YAP/TAZ in mechanotransduction, Nature, 474 (2011) 179. [PubMed: 21654799]

[21]. Halder G, Dupont S, Piccolo S, Transduction of mechanical and cytoskeletal cues by YAP and TAZ, Nature reviews Molecular cell biology, 13 (2012) 591–600.

[22]. Li Z, Bao S, Wu Q, Wang H, Eyler C, Sathornsumetee S, Shi Q, Cao Y, Lathia J, McLendon RE, Hypoxia-inducible factors regulate tumorigenic capacity of glioma stem cells, Cancer cell, 15 (2009) 501–513. [PubMed: 19477429]

[23]. Zhong H, De Marzo AM, Laughner E, Lim M, Hilton DA, Zagzag D, Buechler P, Isaacs WB, Semenza GL, Simons JW, Overexpression of hypoxia-inducible factor 1α in common human cancers and their metastases, Cancer research, 59 (1999) 5830–5835. [PubMed: 10582706]

[24]. Kim J.-w., Tchernyshyov I, Semenza GL, Dang CV, HIF-1-mediated expression of pyruvate dehydrogenase kinase: a metabolic switch required for cellular adaptation to hypoxia, Cell metabolism, 3 (2006) 177–185. [PubMed: 16517405]

[25]. Tsai JH, Yang J, Epithelial–mesenchymal plasticity in carcinoma metastasis, Genes & development, 27 (2013) 2192–2206. [PubMed: 24142872]

[26]. Eramo A, Ricci-Vitiani L, Zeuner A, Pallini R, Lotti F, Sette G, Pilozzi E, Larocca LM, Peschle C, De Maria R, Chemotherapy resistance of glioblastoma stem cells, Cell death and differentiation, 13 (2006) 1238. [PubMed: 16456578]

[27]. Turner JG, Sullivan DM, CRM1-mediated nuclear export of proteins and drug resistance in cancer, Current medicinal chemistry, 15 (2008) 2648–2655. [PubMed: 18991627]

[28]. Henry-Mowatt J, Dive C, Martinou J-C, James D, Role of mitochondrial membrane permeabilization in apoptosis and cancer, Oncogene, 23 (2004) 2850. [PubMed: 15077148]

[29]. Dean M, ABC transporters, drug resistance, and cancer stem cells, Journal of mammary gland biology and neoplasia, 14 (2009) 3–9. [PubMed: 19224345]

[30]. Bleau AM, Huse JT, Holland EC, The ABCG2 resistance network of glioblastoma, Cell Cycle, 8 (2009) 2936–2944. [PubMed: 19713741]

[31]. Kovalev AA, Tsvetaeva DA, Grudinskaja TV, Role of ABC-cassette transporters (MDR1, MRP1, BCRP) in the development of primary and acquired multiple drug resistance in patients with early and metastatic breast cancer, Experimental oncology, (2013) 287–290. [PubMed: 24382439]

[32]. Doye V, Hurt E, From nucleoporins to nuclear pore complexes, Current opinion in cell biology, 9 (1997) 401–411. [PubMed: 9159086]

[33]. Patel SS, Belmont BJ, Sante JM, Rexach MF, Natively unfolded nucleoporins gate protein diffusion across the nuclear pore complex, Cell, 129 (2007) 83–96. [PubMed: 17418788]

[34]. Marcato P, Dean CA, Pan D, Araslanova R, Gillis M, Joshi M, Helyer L, Pan L, Leidal A, Gujar S, Aldehyde dehydrogenase activity of breast cancer stem cells is primarily due to isoform ALDH1A3 and its expression is predictive of metastasis, Stem cells, 29 (2011) 32–45. [PubMed: 21280157]

[35]. Trerotola M, et al., CD133, Trop-2 and α2β1 integrin surface receptors as markers of putative human prostate cancer stem cells, American journal of translational research 2.2 (2010) 135. [PubMed: 20407603]

[36]. Almozyan S, Colak D, Mansour F, Alaiya A, Al-Harazi O, Qattan A, Al-Mohanna F, Al-Alwan M, Ghebeh H, PD-L1 promotes OCT4 and Nanog expression in breast cancer stem cells by sustaining PI3K/AKT pathway activation, International journal of cancer, 141 (2017) 1402–1412. [PubMed: 28614911]

[37]. Gires O, Klein CA, Baeuerle PA, On the abundance of EpCAM on cancer stem cells, Nature Reviews Cancer, 9 (2009) 143–143.

[38]. Pietras A, Katz AM, Ekström EJ, Wee B, Halliday JJ, Pitter KL, Werbeck JL, Amankulor NM, Huse JT, Holland EC, Osteopontin-CD44 signaling in the glioma perivascular niche enhances cancer stem cell phenotypes and promotes aggressive tumor growth, Cell stem cell, 14 (2014) 357–369. [PubMed: 24607407]

[39]. Le Belle JE, Orozco NM, Paucar AA, Saxe JP, Mottahedeh J, Pyle AD, Wu H, Kornblum HI, Proliferative neural stem cells have high endogenous ROS levels that regulate self-renewal and neurogenesis in a PI3K/Akt-dependant manner, Cell stem cell, 8 (2011) 59–71. [PubMed: 21211782]

[40]. ГИПОКСИИ ИП, ACTIVATION OF HYPOXIA-INDUCIBLE FACTOR 1a BY OXYGEN INDEPENDENT PATHWAYS, Экспериментальная онкология, 23 (2001) 88–96.

[41]. Li L, Madu CO, Lu A, Lu Y, HIF-1α promotes a hypoxia-independent cell migration, The open biology journal, 3 (2010) 8. [PubMed: 20882121]

[42]. Bao M, Xie J, Piruska A, Huck WTS, 3D microniches reveal the importance of cell size and shape, Nature communications, 8 (2017) 1–12.

[43]. Zanconato F, Cordenonsi M, Piccolo S, YAP/TAZ at the roots of cancer, Cancer cell, 29 (2016) 783–803. [PubMed: 27300434]

[44]. Zhang X, Zhao H, Li Y, Xia D, Yang L, Ma Y, Li H, The role of YAP/TAZ activity in cancer metabolic reprogramming, Molecular cancer, 17 (2018) 1–10. [PubMed: 29304823]

[45]. Pathak A, Kumar S, Independent regulation of tumor cell migration by matrix stiffness and confinement, Proceedings of the National Academy of Sciences, 109 (2012) 10334–10339.

Highlights

- Physically tight confinement during cancer cell migration triggers therapeutic resistance and induces cancer stem cell-like behavior
- Up-regulating efflux proteins on cell membrane and increasing cancer stem cell related markers after confined-migration contributes to increased therapeutic resistance
- Re-localization of Yes-associated protein (YAP) to the cell nucleus indicated an elevated level of cytoskeletal tension during confined-migration

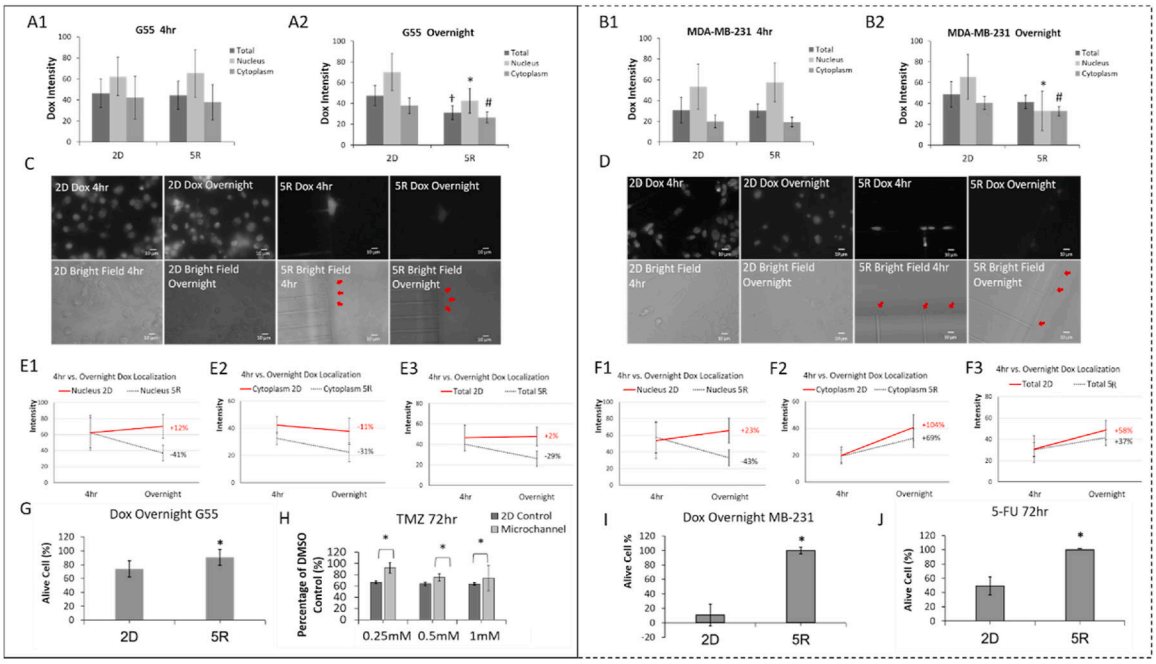

Fig. 1. Confined-migrating cancer cells develop chemotherapeutic resistance by increasing drug efflux

(left panel are G55 results and right panel are MDA-MB-231 results). **A-B.** Quantitative comparison of Dox intracellular accumulation between 2D culture (2D) and cancer cells that migrated through 5 × 5 μm microchannels (5R). Dox (17μM) was introduced to all cancer cells then removed after 4 hours and replaced with the Dox free medium. After overnight incubation with Dox free medium, Dox intensities were quantified in the nucleus, cytoplasm and whole cell (total). N>20 per group. All experiments were triplicated. †$p<0.05$ between 2D total and others; *$p<0.05$ between 2D nucleus and others; #$p<0.05$ between 2D cytoplasm and others. **C-D.** Representative images of Dox accumulation in 2D culture and cells which have migrated through 5 × 5 μm microchannels (red arrows). **E-F.** Changes of Dox intensity over time under different degrees of confinement. Percentage shows intensity changes between 4 hr and overnight. N>20 per group. **G and I.** Viability after Dox (17 μM) 4 hr treatment plus overnight Dox free incubation. N>20 per group. *$p<0.05$ between 2D and others. **H.** G55 cell viability after Temozolomide treatment (0.25 mM, 0.5 mM or 1 mM) for 72 hours. *$p<0.05$. **J.** MDA-MB-231 cell viability after 5-Fu (5 μM) treatment for 72 hours. *$p<0.05$. Experiments were replicated.

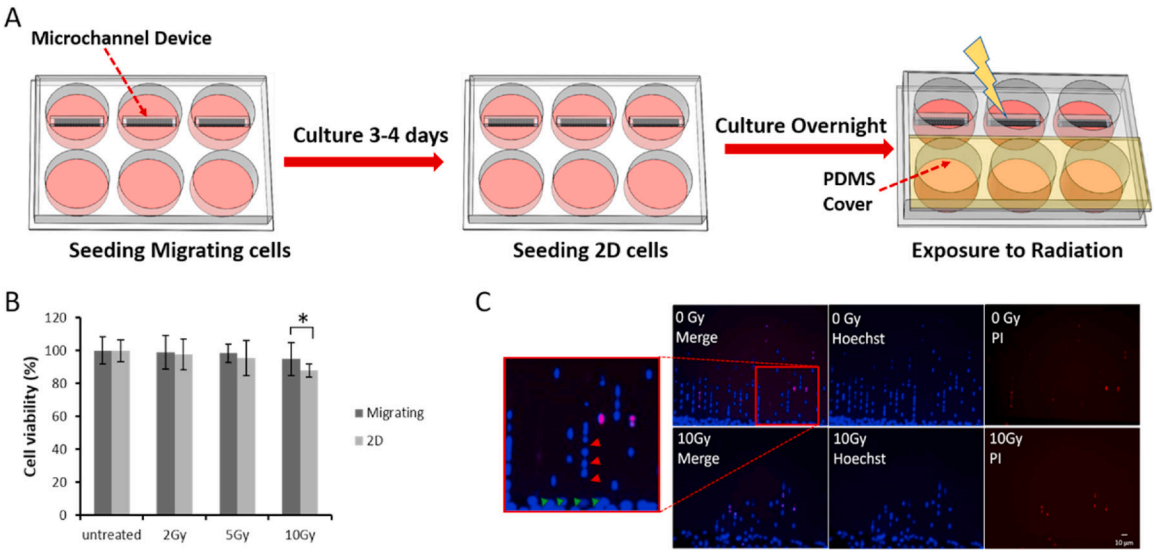

Fig. 2. Confined-migrating cells exhibit more radiation resistance than the 2D cultured cells.

A. G55 cells were seeded and allowed to migrate in 5 μm width microchannel (top row of 6-well plate) and to grow in 2D (bottom row of 6-well plate); then the plate was irradiated in various doses with a PDMS cover on the top of the 2D wells to control for the potential effect of PDMS on viability. **B.** Quantitative comparison of cell viability between 2D and confined-migrating cells at different doses of radiation; average ± Std. *$p<0.05$. $N>20$ images from at least 3 wells for migrating cells per group; $N=6$ for the 2D cultured cells per group. **C.** Representative live/dead images of confined-migrating G55 cells (migrating through 5 × 5 μm microchannels) treated with 0 Gy and 10 Gy radiation. Images were taken 48 hour post-treatment. (Red arrows indicate lined confined-migrating cells inside microchannels; Green arrows indicate 2D cultured cells.)

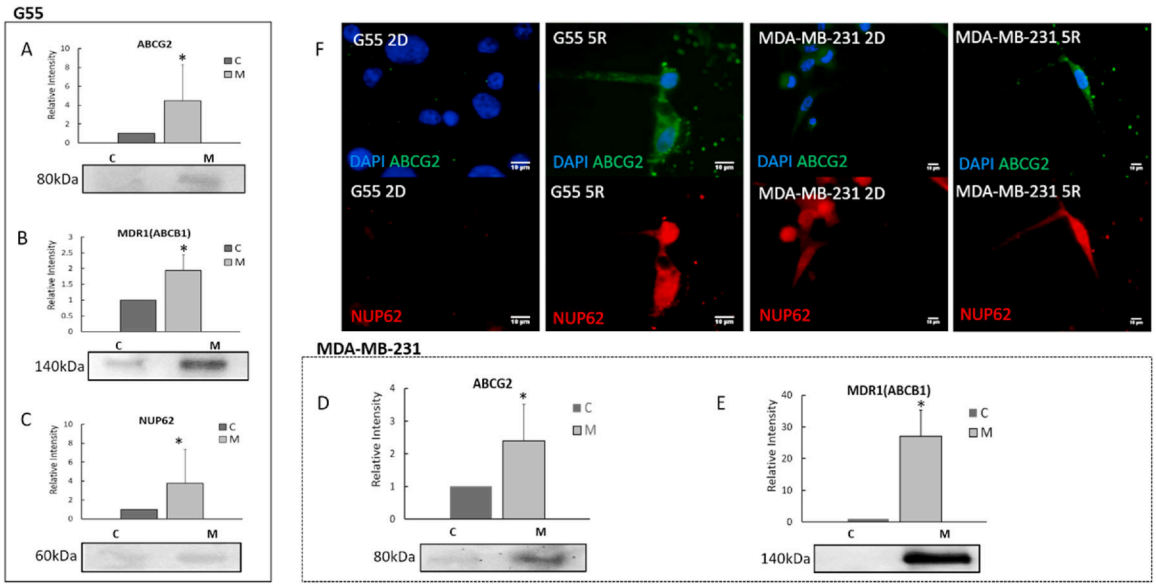

Fig. 3. Confined-migrating cells express significant increased drug efflux proteins.

A-C. Quantitative comparison of drug efflux proteins (ABCG2, MDR1 and NUP62) between G55 confined-migrating cells (indicated by M) and 2D cells (indicated by C). **D-E.** Quantitative comparison of drug efflux proteins (ABCG2 and MDR-1) in MDA-MB-231 confined-migrating cells (indicated by M) and 2D cells (indicated by C). All Western blot results were normalized by the total protein concentration. (Average + Std). All experiments were reproduced. *p<0.05. **F.** Representative immunostaining images of NUP62 and ABCG2 for G55 (left) and MDA-MB-231 cells in 2D culturing and after migrating through 5 × 5 μm microchannels (5R, right). Blue: DAPI; Red: NUP62; and Green: ABCG2.

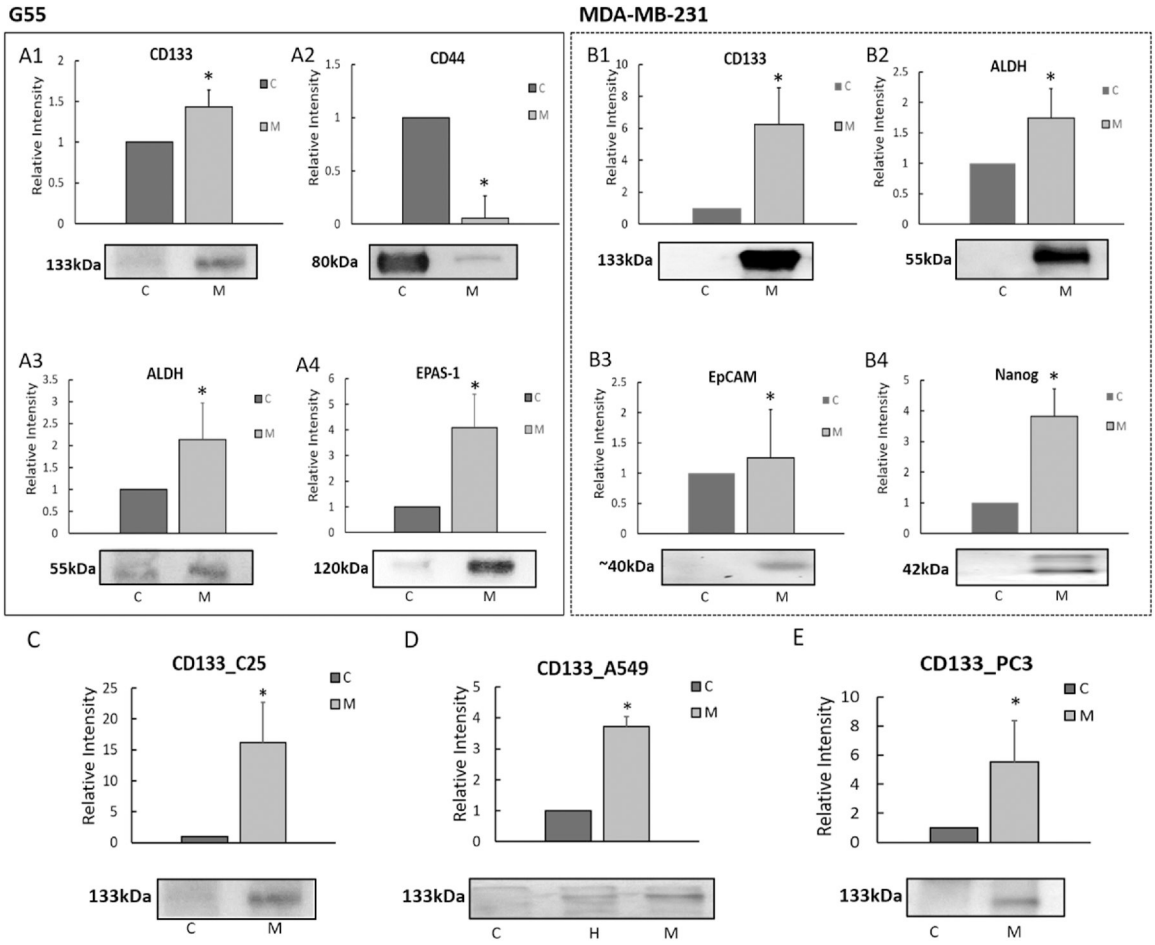

Fig. 4. Increased expression of cancer stem cell related markers in confined-migrating cancer cells.

Quantitative comparison of cancer stem cell related markers using Western blot analyses between confined-migrating (M) and 2D cultured (C) cancer cells. **A1**-**A4**. G55 cells. **B1**-**B4.** MDA-MB-231cells. **C**-**E.** Increased expression of CD133 in different types of confined-migrating cancer cells: C25 patient derived GBM cells, A549 lung cancer cell line, and PC3 prostate cancer cell line. **(**H: hypoxia condition, refer to Fig. S4). All results were normalized as relative intensity to the expression in control group. Average + Std. *p<0.05. All experiments were reproduced. Representative blot images of each marker are shown below their respective graph.

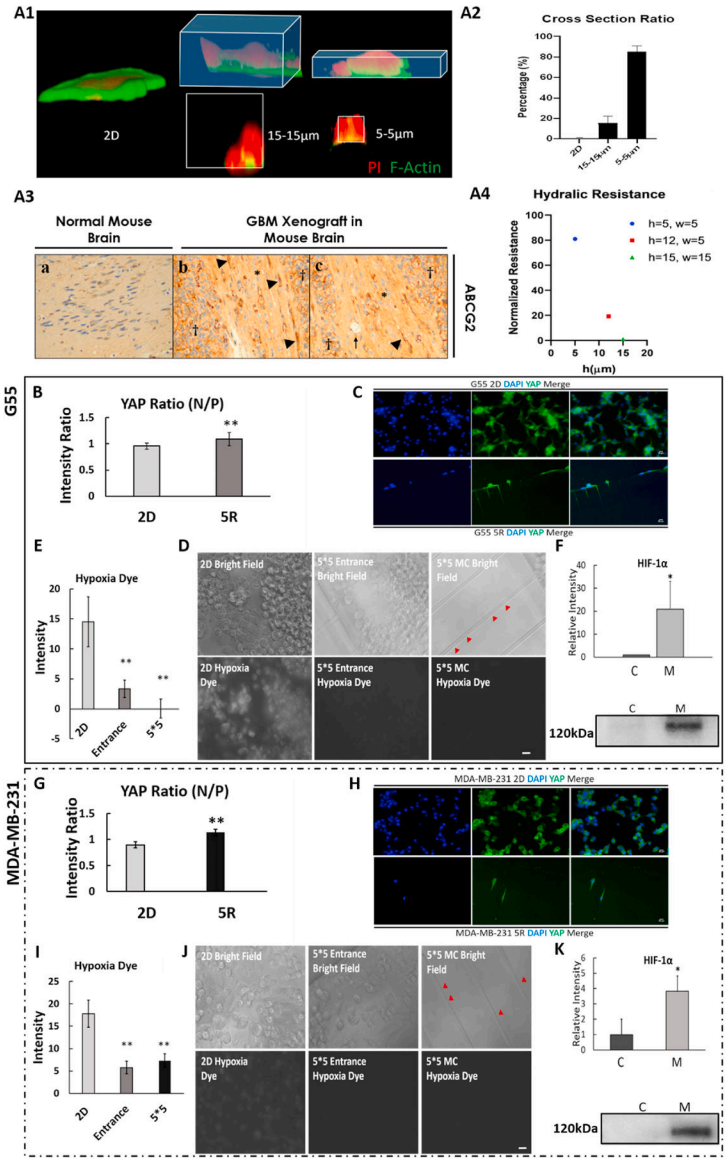

Fig. 5. Confined-migrating cancer cells exhibit increased cytoskeleton tension with minimal hypoxic stress.

A1. 3D reconstructed MDA-MB-231 cells under different degrees of confinement: 2D, 15×15 and 5×5 μm microchannel (Red: PI; Green: F-actin). **A2**. Cross section ratio of MDA-MB-231 cells inside microchannel. Average + Std, n=4/condition. (cross section ratio = cross section acreage of cell/cross section acreage of microchannel) **A3.** Immunohistochemical staining for ABCG2 in the G55 murine xenograft model of glioblastoma multiforme demonstrates high ABCG2 expression in migrating tumor cells within cortical white matter tracts. a: health mouse brain tissue (noncancerous). b-c: In areas bordering G55 tumors (labeled with †), elevated ABCG2 expression can be observed in the migrating tumor cells within cortical white matter tracts (labeled with*). Arrow: blood vessel. Arrowhead: tumor cells highly expressing ABCG2 in a whole cell pattern. **A4.** Hydraulic resistance inside microchannels with different dimensions. h: height; w: width. Results are normalized by the lowest resistance number (i.e., 15×15 μm microchannel). **B**

and **G.** Quantitative comparison of YAP expression (N/P; nucleus/cytoplasm) between 2D cultured and confined-migrated cells. 5R: cells migrated through 5 × 5 μm microchannel. **C** and **H.** Representative YAP fluorescence images of G55 (**C**) and MDA-MB-231 (**H**) cells. Blue: DAPI; Green: YAP. Scale bar: 10μm. **D** and **J**. Representative hypoxia dye fluorescence images of cells in the central reservoir (2D), 5 × 5 μm entrance and inside 5 × 5 μm microchannels (MC). Red arrows indicate the confined-migrating cells via the 5 × 5 μm microchannels. **E** and **I.** Quantitative comparison of hypoxia dye intensity of the cells in different locations. **F** and **K**. Western blot HIF-1α relative intensity. C: 2D cultured cells and M: cells migrated through 5 × 12 μm microchannels. All results were normalized to the total proteins. Average + Std. *$p<0.05$, **$p<0.01$ between 2D and others. Scale bar: 5 μm. All experiments were reproduced.

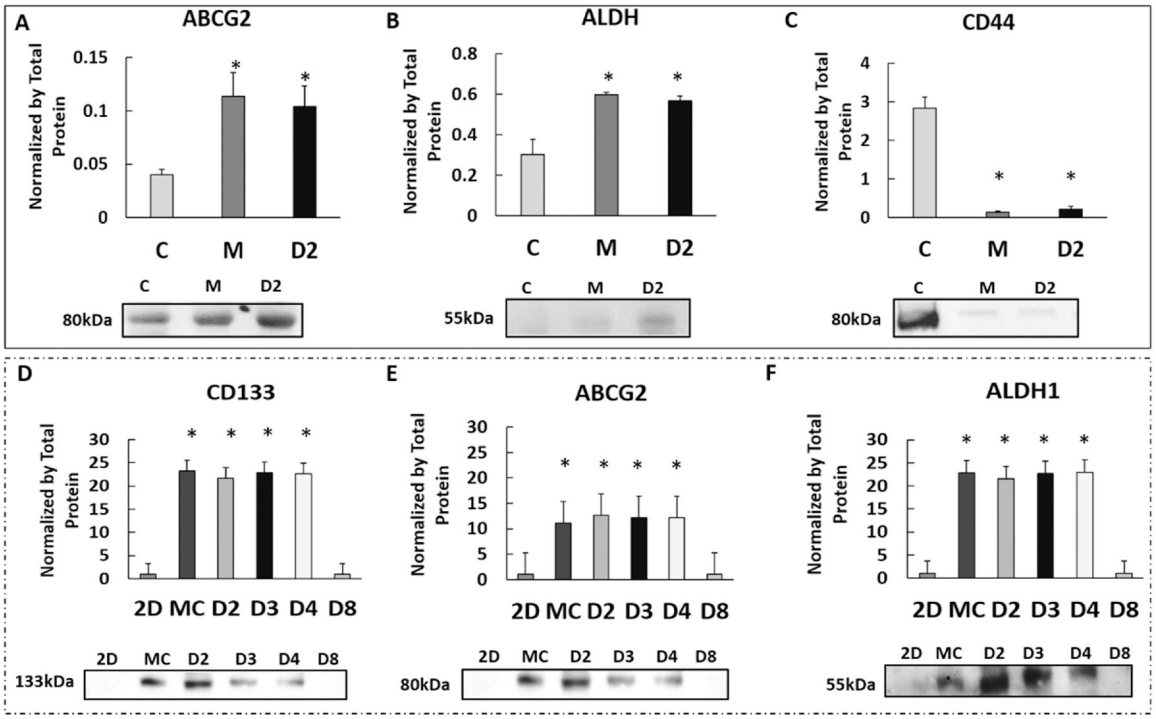

Fig 6. Protein expression changes induced by confined-migration persist after removal from physical confinement.

A-C. Comparison of selected proteins (ABCG2, ALDH and CD44) expression in G55 cells between 2D culture (2D), confined-migrating (M), and 2 days after reseeding confined-migrating cells on the 2D culture (D2). **D-F.** Comparison expressions of selected proteins (CD133, ABCG2 and ALDH1) in MDA-MB-231 cells between 2D culture (2D), confined-migrating (M), and 2, 3, 4, and 8 days after reseeding confined-migrating cells (D2, D3, D4, and D8). Representative blot images of each marker are shown below their respective graphs. All results were normalized to the total proteins. Average + Std. *$p<0.05$. All experiments were reproduced.